

THE “WATER-FOUNTAIN NEBULA” IRAS 16342–3814: *HUBBLE SPACE TELESCOPE*/VERY LARGE ARRAY STUDY OF A BIPOLAR PROTOPLANETARY NEBULA

RAGHVENDRA SAHAI,¹ PETER TE LINTEL HEKKERT,² MARK MORRIS,³ ALBERT ZIJLSTRA,⁴ AND LAUREN LIKKEL⁵

Received 1998 December 15; accepted 1999 January 29; published 1999 February 00

ABSTRACT

We present *Hubble Space Telescope* (*HST*) Wide-Field Planetary Camera 2 images and VLA OH maser emission-line maps of the cold infrared object IRAS 16342–3814, believed to be a protoplanetary nebula. The *HST* images show an asymmetrical bipolar nebula, with the lobes separated by a dark equatorial waist. The two bright lobes and the dark waist are simply interpreted as bubble-like reflection nebulae illuminated by starlight escaping through polar holes in a dense, flattened, optically thick cocoon of dust, which completely obscures the central star. A faint halo can be seen surrounding each of the lobes. The bubbles are likely to have been created by a fast outflow (evidenced by H₂O emission) plowing into a surrounding dense, more slowly expanding, circumstellar envelope of the progenitor asymptotic giant-branch (AGB) star (evidenced by the halo). The *IRAS* fluxes indicate a circumstellar mass of about $0.7 M_{\odot} (D/2 \text{ kpc})$ and an AGB mass-loss rate of about $10^{-4} M_{\odot} \text{ yr}^{-1} (V_{\text{exp}}/15 \text{ km s}^{-1})(D/2 \text{ kpc})^2$ (assuming a gas-to-dust ratio of 200). OH features with the largest redshifted and blueshifted velocities are concentrated around the bright eastern and western polar lobes, respectively, whereas intermediate-velocity features generally occur at low latitudes, in the dark waist region. We critically examine evidence for the post-AGB classification of IRAS 16342–3814.

Subject headings: circumstellar matter — planetary nebulae: general — stars: AGB and post-AGB — stars: mass loss

1. INTRODUCTION

The “water-fountain nebula,” IRAS 16342–3814 (hereafter IRAS 1634; also OH 344.1+5.8) belongs to a class of unusual evolved stars with high-velocity outflows traced in either or both of radio H₂O and OH maser line emission (Likkell & Morris 1988, hereafter LM88; te Lintel Hekkert et al. 1988). IRAS 1634 is believed to be in the short-lived *protoplanetary* (PPN) phase of stellar evolution based on its cold infrared spectral energy distribution and high-velocity bipolar outflow implied by the maser line data (LM88; Likkell, Morris, & Madalena 1992, hereafter LMM92). High-resolution imaging of young post-asymptotic giant branch (PAGB) objects like IRAS 1634 (e.g., Kwok, Hrivnak, & Su 1998; Su et al. 1998; Sahai et al. 1999) is necessary for a detailed understanding of their structure, eventually leading to a resolution of the long-standing issue of how aspherical planetary nebulae are formed. However, most PPNs are small in angular extent and, at best, poorly resolved with ground-based telescopes (Hrivnak et al. 1999). Thus, although the maser emission observations strongly indicate a bipolar morphology for IRAS 1634, direct evidence (i.e., imaging) has been lacking. In this Letter, we report *Hubble Space Telescope* (*HST*) and Very Large Array (VLA) observations that dramatically reveal IRAS 1634’s bipolar spatio-kinematic structure.

2. OBSERVATIONS AND RESULTS

The *HST* archival images of IRAS 1634 were taken with the 800×800 pixel planetary camera of Wide-Field Planetary Camera 2 (WFPC2), which has a plate scale of $0''.0456 \text{ pixel}^{-1}$ (Trauger et al. 1994), using the F555W [$\langle \lambda \rangle = 0.55 \mu\text{m}$, $\Delta\lambda = 0.123 \mu\text{m}$; exposures were $3 \times (1, 10, \text{ and } 100) \text{ s}$] and F814W [$\langle \lambda \rangle = 0.80 \mu\text{m}$, $\Delta\lambda = 0.149 \mu\text{m}$; exposures were $3 \times (1 \text{ and } 10) \text{ s}$, and $2 \times 100 \text{ s}$] filters. Using the VLA in its A configuration (angular resolution of $2''$), the OH 1612 (1665/1667) MHz lines were observed in IRAS 1634 on 1990 August 15 (1988 October 30) with a velocity resolution of $0.55 (8.8) \text{ km s}^{-1}$; the rms noise per channel was $25 (9) \text{ mJy}$. A search for millimeter-wave molecular line emission from IRAS 1634 with the Swedish-ESO Submillimeter Telescope, La Silla, Chile (Booth et al. 1989) during 1989 September gave null results—the 5σ noise levels in the 0.7 MHz resolution CO $J = 1-0$ and $2-1$ spectra (on the chopper-corrected antenna temperature T_A^* scale) were 0.014 and 0.05 K , respectively. Since the line widths for IRAS 1634 are expected to be $\geq 30 \text{ km s}^{-1}$ (§ 5), the upper limits on T_A^* are a factor of ≥ 3 more sensitive than the above noise levels.

Both the F555W and F814W images (Fig. 1a) show a bipolar nebula with its long axis aligned along P.A. = 73° . The J2000 coordinates of the peak intensity points in the western and eastern lobes respectively are $\alpha = 16^{\text{h}}37^{\text{m}}39^{\text{s}}.89$, $\delta = -38^\circ20'17''.4$ and $\alpha = 16^{\text{h}}37^{\text{m}}40^{\text{s}}.02$, $\delta = -38^\circ20'16''.9$, in good agreement with the ground-based near-IR position $\alpha = 16^{\text{h}}37^{\text{m}}40^{\text{s}} \pm 0.1$, $\delta = -38^\circ20'14''.3 \pm 1$ (van der Veen, Habing, & Geballe 1989, hereafter VH89). The two lobes are separated by a dark waist. The western lobe is brighter than the eastern one by factors of 13 and 6.8 in F555W and F814W, respectively. Using the WFPC2 calibration given by Holtzman et al. (1995), we find from our *HST* images $m_v = 15.7$ and $m_i = 13.15$ for the whole nebula and $m_v = 15.8 (18.6)$ and $m_i = 13.3 (15.5)$ for the western (eastern) lobes. Thus, the eastern lobe is significantly redder than the western one. Although the nebula looks roughly axisymmetric, the individual

¹ Jet Propulsion Laboratory, MS 183-900, California Institute of Technology, Pasadena, CA 91109.

² Australia Telescope National Facility, P.O. Box 76, Epping, NSW 2121, Australia.

³ Division of Astronomy and Astrophysics, UCLA, Los Angeles, CA 90095-1562.

⁴ University of Manchester Institute of Science and Technology, Department of Physics, P.O. Box 88, Manchester M60 1QD, UK.

⁵ Department of Physics and Astronomy, University of Wisconsin–Eau Claire, Eau Claire, WI 54702-4004.

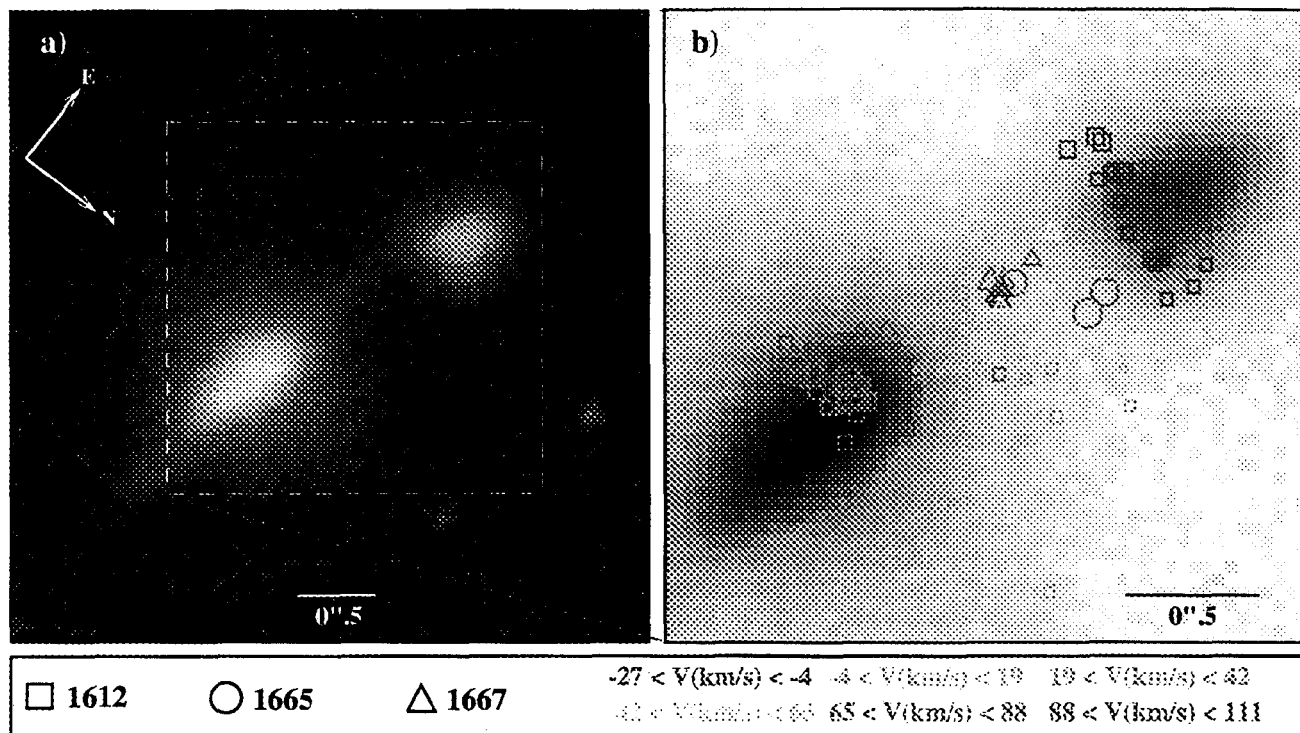


FIG. 1.—(a) Color image of the protoplanetary nebula IRAS 16342–3814, made of exposures taken with *HST*/WFPC2 through the F814W (in red) and F555W (in green) filters and displayed on a logarithmic stretch. A faint reddish halo surrounds the bright yellow lobes. The linear protrusions emerging from the bright west lobe at 45° to the horizontal axis are diffraction artifacts caused by telescope optics. (b) VLA OH 1612, 1665, and 1667 MHz maser line features, overlaid on the F814W image (in gray scale). The positions of the features were obtained by Gaussian fitting, yielding positions to better than 20% of the $2''$ beam size. The OH features have been grouped into six color-coded velocity bins. The symbol sizes are proportional to the square root of the integrated flux. The highest flux features have strengths of 8.83, 0.53, and 1.17 Jy for the 1612, 1665, and 1667 MHz lines, respectively.

symmetry axes of each lobe do not coincide. The orientation of the teardrop-shaped lobes and their location vis-à-vis the dark waist are centrally point-symmetric in detail. We have verified this by scaling the west-lobe intensity to match that of the east lobe, rotating it by 180° around the nebular center (defined as the average of the peak intensity locations in each lobe) and subtracting it from the east lobe; the residual is very small.

The OH 1612, 1665, and 1667 MHz data are shown overlaid

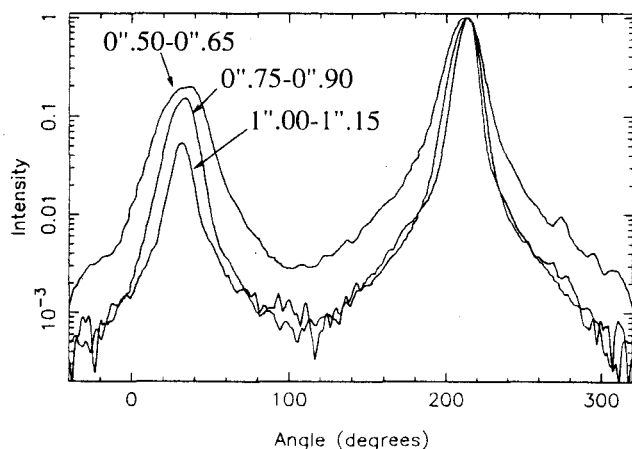


FIG. 2.—Average intensity in the F814W image along an annulus centered at the nebular center in the F814W image, for three different annuli (inner/outer radii of the annuli are labelled). The maximum average intensity in each annulus has been normalized to unity.

on the *HST* F814W image (gray scale) in Figure 1b. The kinematic center of symmetry of each OH data set was assumed to coincide with the center of the optical nebula. Taking the systemic velocity to be $42 \pm 2 \text{ km s}^{-1}$, the extreme redshifted and blueshifted 1612 MHz emission features are found to occur in two clusters spatially separated along an axis roughly co-aligned with the optical axis of the nebula. The blueshifted (redshifted) maser spots are associated with the brighter (fainter) visible lobe, implying that the nebular axis is tilted such that the brighter western lobe is nearer to us.

The emission blueward of the systemic velocity is significantly stronger than the redshifted emission, suggesting that the former includes a contribution from amplified continuum emission, presumably due to shock-ionized gas in the lobes.

Faint halos can be discerned around the lobes, suggesting that these are regions illuminated by scattered light from the bright lobes. Azimuthal cuts in the F814W image taken around the nebular center (Fig. 2) shows that the nebular intensity first falls very steeply from the center to the edge of the lobes and then more slowly in the halo. The color of the halos is significantly redder than that of the bright lobes—e.g., the ratios of the counts per second in the F814W to F555W images is 2.9 (5.6) for the brightest (i.e., with 75%–100% of the peak lobe intensity) region of the west (east) lobe compared to 5.6 (7.3) for the west (east) halo (region surrounding lobe with 2%–5% of the peak lobe intensity). If the halo is illuminated by the bright lobes, then (assuming that each lobe is roughly cylindrically symmetric around some nominal nebular axis), the light from the halo, compared to the light from the lobes, has undergone (1) “blueing” because of the second scattering and (2) additional “reddening” because it traverses a longer

On the basis of spectra alone, LM88 suggested that the OH masers in IRAS 1634 arise at intermediate systemic latitudes, at which the outflow velocity is presumed to be much less than along the polar axis, by analogy with the related bipolar nebula OH 231.8+4.2 (Morris et al. 1987). Figure 1b is consistent with that expectation. Many of the weaker spots appear to arise from the vicinity of the equatorial dust cocoon, while the rest appear to gird the optical lobes. We suggest that the 1612 MHz maser emission seen projected on the lobes arises in the enhanced-density and/or shocked boundaries of the latter. The velocity offset of the OH features from the systemic velocity, plotted as a function of projected distance from the center of the nebula, shows a strong gradient (Fig. 3). The greater spread in the polar angles of the lower velocity features (Fig. 1b) implies that these represent outflowing gas at relatively lower latitudes at a variety of longitudinal angles. The observed gradient is thus consistent with the idea that the outflow velocity increases from low to high latitudes. Following LM88 and LMM92, we suggest that the high-velocity (up to 130 km s^{-1}) H_2O masers lie near the polar axis at which the outflow velocity is likely to be largest; these masers may be expected to arise in the postshock region in which the high-velocity flow interacts with the ambient dense AGB CSE. Direct observation of the locations of the H_2O masers would be of considerable value for interpreting the high-velocity flow.

5. THE PROGENITOR AGB STAR: NEUTRAL NEBULAR MASS AND MASS-LOSS RATE

We have fitted the *IRAS* far-infrared fluxes of IRAS 1634 to estimate the mass of warm dust (as, e.g., in Sahai et al. 1991). Assuming that the total luminosity of IRAS 1634 is typical of late-AGB/early-PAGB stars, i.e., $\sim 6000 L_\odot$, we estimate its distance D to be 2 kpc—a reasonable value considering its $5^\circ 8$ galactic latitude—and a scale height of 150 pc appropriate for a $\sim 2 M_\odot$ progenitor star. S1 is probably not a significant contributor to the far-IR fluxes of IRAS 1634 because the probability of finding two evolved stars with heavy mass loss so close to each other at $5^\circ 8$ galactic latitude is very low. Assuming a λ^{-p} power-law dust emissivity of $150 \text{ cm}^2 \text{ g}^{-1}$ at $60 \mu\text{m}$ (Jura 1986), we find a good fit to the color-corrected *IRAS* fluxes (130.4, 264.4, 224.5, and 18.4 Jy in the 100, 60, 25, and $12 \mu\text{m}$ bands, respectively), using two dust components with masses and temperatures, respectively, of 2.3×10^{-3} (4.5×10^{-3}) and 1.6×10^{-7} (1.5×10^{-7}) M_\odot and 100 (84) and 468 (422) K, for $p = 1$ (1.5). Thus, the total mass of circumstellar matter M_{env} in IRAS 1634 is rather large: about $(0.5\text{--}0.9) M_\odot$ assuming a typical gas-to-dust ratio of 200 for AGB CSEs.

The characteristic radius of the far-infrared dust-emitting region r_d is unknown. If the dust is heated by starlight, then $r_d = (L_* T_*^p / 16\pi\sigma)^{1/2} T_d^{-(2+p/2)}$ (Sopka et al. 1985; Herman, Bur-

ger, & Penninx 1986), giving $T_d = 84 \text{ K}$ at $r_d = (2.1\text{--}4.9) \times 10^{17} \text{ cm}$ for $T_* = (3500\text{--}10,000) \text{ K}$ and $p = 1.5$. Thus, from the dust ejection timescale $t_{\text{exp}} \sim (0.44\text{--}1) \times 10^4 \text{ yr}$ derived assuming a typical expansion velocity of $V_{\text{exp}} = 15 \text{ km s}^{-1}$, we find a progenitor AGB mass-loss rate of $\dot{M} = M_{\text{env}}/t_{\text{exp}} \sim 10^{-4} (V_{\text{exp}}/15 \text{ km s}^{-1}) M_\odot \text{ yr}^{-1}$. If $p = 1$ or if the starlight is significantly reddened, \dot{M} is higher, because r_d is significantly smaller. The following proportionalities apply: $M_{\text{env}} \propto D^2$ and $\dot{M} \propto D$. Thus, in spite of the large uncertainties in the above derivation, our derived mass-loss rate lies at the upper end of the range observed for AGB red giants (e.g., Loup et al. 1993).

The lack of CO emission in IRAS 1634 (§ 2) is not surprising, considering that many PPNs are relatively weak in CO emission (Bujarrabal & Bachiller 1991), and probably results from relatively kinetic low temperatures in its CSE—an explanation supported by theoretical modeling (Jura, Kahane, & Omont 1988; Sahai 1990) and observations (Sahai 1997). IRAS 1634 shows no evidence for photoionized gas, indicating that its central star has not yet reached the planetary nebula phase. It shows many similarities to M1–92 (Bujarrabal et al. 1998), in morphology, broad main-line OH emission (Seaquist, Plume, & Davis 1991), and the presence of the $3.1 \mu\text{m}$ ice absorption band (VHG89; Eiroa & Hodapp 1989) caused by grains with ice mantles. The morphology of M1–92 may be somewhat more evolved than IRAS 1634, and it may have left the AGB earlier.

6. IRAS 1634 AND THE FORMATION OF ASPHERICAL PLANETARY NEBULAE

A recent imaging survey of very young planetary nebulae shows that all objects display aspherical structure, including multiple bubbles and jets with a large degree of point symmetry (Sahai & Trauger 1998, hereafter ST98). ST98 hypothesize that fast collimated outflows with changing directionality are the primary agent for setting the stage in the formation and shaping of planetary nebulae, rather than a preexisting equatorial density enhancement in the AGB CSE, as assumed in the popular generalized interacting winds (GISW) model (Balick 1987). The GISW model produces bipolar shapes with reflection symmetry about the equatorial plane and cylindrical symmetry around an axis orthogonal to the equatorial plane; hence, it cannot easily explain point-symmetric morphology. IRAS 1634 shows strong evidence for two important components of ST98's hypothesis: (1) a collimated high-velocity wind, shaping a (2) point-symmetric imprint on the surrounding dense AGB CSE. Further detailed studies of this important transition object are clearly warranted.

R. S. and M. M. are thankful for partial financial support for this work provided by NASA through a Long-Term Space Astrophysics grant.

REFERENCES

- Balick, B. 1987, *AJ*, 94, 671
 Bedijn, P. J. 1987, *A&A*, 136, 186
 Booth, R. S., et al. 1989, *A&A*, 216, 315
 Bujarrabal, V., Alcolea, J., Sahai, R., Zamorano, J., & Zijlstra, A. A. 1998, *A&A*, 331, 361
 Bujarrabal, V., & Bachiller, R. 1991, *A&A*, 242, 247
 Eiroa, C., & Hodapp, K.-W. 1989, *A&A* 223, 271
 Herman, J., Burger, J. H., & Penninx, W. H. 1986, *q9*
 Holtzman, J. A., Burrows, C. J., Casertano, S., Hester, J. J., Trauger, J. T., Watson, A. M., & Worthey, G. 1995, *PASP*, 107, 1065
 Hrivnak, B. J., Kwok, S., & Volk, K. M. 1989, *ApJ*, 346, 265
 Hrivnak, B. J., Langill, P. P., Su, K. Y. L., & Kwok, S. 1999, *ApJ*, 513, 421 *q10*
 Jura, M. 1986, *ApJ*, 303, 327
 Jura, M., Kahane, C., & Omont, A. 1988, *A&A*, 201, 80
 Kwok, S., Hrivnak, B. J., & Su, K. Y. L. 1998, *ApJ*, 501, L117
 Likkell, L., & Morris, M. 1988, *ApJ*, 329, 914
 Likkell, L., Morris, M., & Maddalena, R. J. 1992, *A&A*, 256, 581
 Loup, C., Forveille, T., Omont, A., & Paul, J. F. 1993, *A&AS*, 99, 291
 Morris, M., Guilloteau, S., Lucas, R., & Omont, A. 1987, *ApJ*, 321, 888
 Olmon, F. M., et al. 1986, *A&AS*, 65, 607
 Sahai, R. 1990, *ApJ*, 362, 652 *q11*
 ———. 1997, *ApJ*, 487, L155

geometric path. The redder color of the halo then implies that effect (2) dominates. Alternatively, the halo region may be dominantly illuminated by heavily reddened, direct starlight.

3. THE NATURE OF THE CENTRAL STAR

Bipolar reflection nebulae are seen around both *evolved* and *pre-main-sequence* (PMS) stars. However, we believe that IRAS 1634 is unlikely to be a PMS object because (1) its systemic velocity is of opposite sign to that of H I in the galactic quadrant in which it is located, and (2) it has no strong, narrow, CO emission which is commonly seen toward PMS objects. Is the IRAS 1634 central star on the asymptotic giant branch (AGB), or is it more evolved? The star is not visible in the *HST* images, and we cannot derive a reliable stellar temperature from the color of the nebulosity because of the competing effects of unknown amounts of reddening due to extinction and blueing due to scattering. VH89 find that fitting the optical ground-based photometry (done with a 15" aperture) gives a stellar temperature $T_* = 17,000$ K, whereas their detection of strong 2.3 μ m CO absorption (using a 5" aperture) implies $T_* \leq 3500$ K. In addition, the *HST* data gives m_V of 15.66 for IRAS 1634, significantly fainter than VH89's value (13.65). These discrepancies may be caused by two bright stars (hereafter S1 and S2), respectively located 9".3 and 11".6 from IRAS 1634 and with *V*- and *I*-magnitudes of (14.9, 11.1) and (13.9, 12.8), contaminating the optical ground-based data.

We believe that IRAS 1634 is a very young PAGB object for the following reasons. First, the 2.3 μ m CO absorption (VH89) may have a significant contribution from dense circumstellar material (which is clearly present in IRAS 1634), so it does not constrain T_* . The probability of variability (i.e., the *IRAS* variability index) is very low for IRAS 1634 (6%), in contrast to the value ($\geq 30\%$) for the vast majority of AGB stars. The *IRAS* Low-Resolution Spectrometer (LRS) spectrum of IRAS 1634 is even redder than for the "extreme AGB" objects OH 231.8+4.2 and OH 17.7-2.0 (Olnon et al. 1986; Bedijn 1987). Bedijn's extensive modeling of the near-to-far-IR spectral energy distribution in evolved stars shows that the very red spectra of objects like OH 17.7-2.0 (and by analogy, IRAS 1634) imply a lack of hot dust near the star, suggesting termination of the heavy AGB mass-loss phase a few times 100 yr ago. Less than 1% of the 5449 objects in the LRS Atlas (Olnon et al. 1986) have a red spectrum like IRAS 1634; the few (≤ 10) such objects for which spectral types have been determined are classified as F, G, K, or A, appropriate for young PAGB stars (e.g., Hrivnak, Kwok, & Volk 1989).

4. THE STRUCTURE OF IRAS 1634

The two bright lobes seen in the *HST* image of IRAS 1634 are simply interpreted as reflection nebulae illuminated by starlight escaping through polar holes in an optically thick, dense, flattened cocoon of dust. The cocoon, seen as the dark waist separating the two lobes, completely obscures the central star from our view. Assuming $T_* \sim 3500$ –10,000 K, we set 3 σ lower limits of 15.5–16.1 (14.8–14.7) on the total extinction optical depth to the central star at 0.55 (0.8) μ m from the absence of a point source in the waist region. The surface brightness falls exponentially across the boundaries of the lobes, both radially and azimuthally, as has been found for the well-studied bipolar PPNs CRL 2688 and Roberts 22 (Sahai et al. 1998a, 1998b; Sahai et al. 1999). By analogy with these objects, it is likely that these sharp lobe edges demarcate optically thick, enhanced-density boundaries of bubbles created

by a fast collimated outflow (evidenced by high-velocity H₂O and OH emission) expanding inside a dense, slowly expanding circumstellar envelope (CSE) of the progenitor AGB star. The enhanced densities at the bubble boundaries thus result from material in the CSE swept up by the fast outflow. Imaging at near-IR wavelengths (e.g., 2–5 μ m), where the optical depths would be lower, is needed to directly confirm the proposed structure of these bubbles. The presence of the dense AGB CSE which constrains the expansion of the fast outflow is revealed by the faint halos around the bright lobes.

The western and eastern lobes are spatially well separated, clearly showing that we are not viewing IRAS 1634 directly along the bipolar outflow axis. Inspection of the OH data presented here led LMM92 to a similar conclusion, contrary to earlier suggestions that the outflow was seen pole-on (LM88; te Lintel Hekkert et al. 1988). Given the $\sim 40^\circ$ observed angular width of the lobes, the inclination i is less than 70° because neither lobe shows 1612 MHz features at or near the systemic velocity. We can estimate i if we assume that the observed velocity spread in the 1612 MHz emission features clustered around the base of each lobe, ΔV_{lobe} (Fig. 1b), is comparable to the difference in projected radial velocities of the front and back sides of the lobe. Then, $\tan i \sin i \sim \{(\Delta V_{\text{lobe}} / [(2V_{\text{end}} - \Delta V_{\text{lobe}}) \tan \phi_o])\}$, where ϕ_o is the *observed* lobe half-opening angle (larger than the *intrinsic* half-opening angle ϕ_i by $1/\sin i$) and V_{end} is the maximum *observed* expansion velocity (smaller than the *intrinsic* expansion velocity by $1/\sin i$). Since the observed ΔV_{lobe} is 11 and 23 km s⁻¹, respectively, for the east and west lobes and $V_{\text{end}} \sim 67$ km s⁻¹, we find $i \sim 40^\circ$. The inclination of the nebular axis can explain the unequal brightnesses of the lobes, assuming the latter to be intrinsically equally bright if one or both of the following conditions are present: (1) attenuation in the outer regions of an overdense equatorial region and (2) a strongly forward-scattering phase function. The bright lobes are very young structures—dividing half the deprojected separation between the most prominent redshifted and blueshifted OH maser emission features ($1''5/\sin i$) by a deprojected OH outflow velocity of 67 km s⁻¹/cos($i - \phi_i$), we get an expansion timescale of 50($D/2$ kpc) yr (the trigonometric factor is ~ 1) for material in the lobes associated with the OH emission.

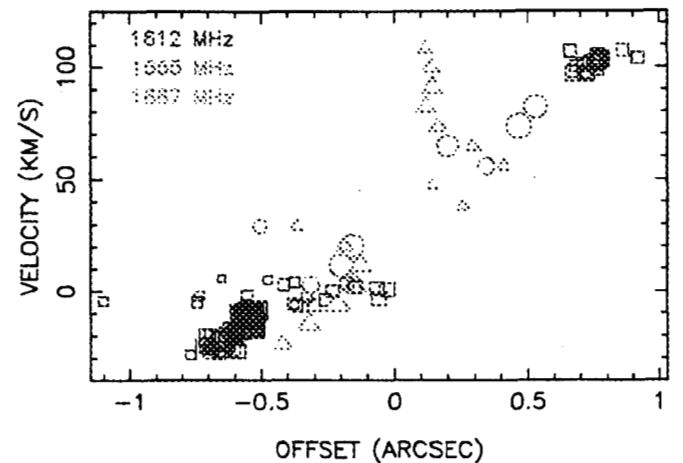


FIG. 3.—Velocity offset of the OH maser features from the systemic velocity (42 km s⁻¹) as a function of distance from center. Distances for which the radial velocity is smaller (larger) than the systemic velocity are located towards the western (eastern) lobes, and are plotted as negative (positive). The integrated flux of each feature corresponds to the size of its symbol as in Fig. 1b.

- Sahai, R., Hines, D. C., Kastner, J. H., Weintraub, D. A., Trauger, J. T., Rieke, M. J., Thompson, R. I., & Schneider, G. 1998a, *ApJ*, 492, L163
- Sahai, R., & Trauger, J. T. 1998, *AJ*, 116, 1357
- Sahai, R., Wootten, A., Schwarz, H. E., & Clegg, R. E. S. 1991, *A&A*, 251, 560
- Sahai, R., et al. 1998b, *ApJ*, 493, 301
- q12 Sahai, R., Zijlstra, A., Bujarrabal, V., & Lintel Hekkert, P. 1999, *AJ*, in press
- Sequist, E. R., Plume, R., & Davis, L. E. 1991, *ApJ*, 367, 200
- Sopka, R. J., Hildebrand, R., Jaffe, D. T., Gatley, I., Roellig, T., Werner, M., Jura, M., & Zuckerman, B. 1985, *ApJ*, 294, 242
- Su, K. Y. L., Volk, K., Kwok, S., & Hrivnak, B. J. 1998, *ApJ*, 508, 744
- te Lintel Hekkert, P., Habing, H. J., Caswell, J. L., Norris, R. P., & Haynes, R. F. 1988, *A&A*, 202, L19
- Trauger, J. T., et al. 1994, *ApJ*, 435, L3
- van der Veen, W. E. C. J., Habing, H. J., & Geballe, T. R. 1989, *A&A*, 226, 108

QUERIES TO THE AUTHOR

1 Au: "PPN" is usually used to stand for "protoplanetary nebula." Is that what you meant?

2 Au: We need to expand WFPC2 the first time it's used. Revisions here OK? (Or is "planetary camera of...Planetary Camera 2" redundant?)

3 Au: Did you mean "These discrepancies may be caused by two bright stars"? Or would "These discrepancies may be because of two bright stars" be better?

4 Au: Correct expansion of LRS?

5 Au: Should it be "ambient dense AGB CSEs" (i.e., more than one CSE)?

6 Au: Revisions here OK?

7 Au: What unit does "g" stand for? Gram? Groove? Please explain.

8 Au: "in the AGB CSEs"?

9 Au: Please complete this entry.

10 Au: Please confirm.

11 Au: This should be listed by the actual authors' names, since "IRAS Science Team" is not the first author (or even included in the official author list per ADS).

12 Au: Published yet?